

A STUDY OF GAS DYNAMICS UNDER POISEUILLE CONDITIONS:
A COMPARISON OF THE FLUID EQUATIONS AND DSMC

by

Charles Nathan Woods

A senior thesis submitted to the faculty of

Brigham Young University

in partial fulfillment of the requirements for the degree of

Bachelor of Science

Department of Physics and Astronomy

Brigham Young University

April 2008

Copyright © 2008 Charles Nathan Woods

All Rights Reserved

BRIGHAM YOUNG UNIVERSITY

DEPARTMENT APPROVAL

of a senior thesis submitted by

Charles Nathan Woods

This thesis has been reviewed by the research advisor, research coordinator,
and department chair and has been found to be satisfactory.

Date

Ross L. Spencer, Advisor

Date

Eric Hintz, Research Coordinator

Date

Ross L. Spencer, Chair

ABSTRACT

A STUDY OF GAS DYNAMICS UNDER POISEUILLE CONDITIONS: A COMPARISON OF THE FLUID EQUATIONS AND DSMC

Charles Nathan Woods

Department of Physics and Astronomy

Bachelor of Science

We have analyzed the flow of a gas through a cylindrical tube of constant radius for Mach number $\ll 1$ using both the fluid equations and direct-simulation-monte-carlo (DSMC). We find that the two methods are in good agreement, and we find that the flow velocity approximately obeys the equation

$$u_z = -\frac{\Delta P}{\Delta z} \frac{1}{4\bar{\mu}} (R^2 - r^2 + 2.2R\lambda) \left[1 - \frac{\Delta n}{\Delta z} \frac{z}{n_0} \right].$$

ACKNOWLEDGMENTS

I would like to recognize the many hours of work put in by the rest of my research group, who got the FENIX program running in the first place, as well as the Department of Energy, for funding my work. I'd especially like to thank Dr. Spencer, whose work on the perturbative expansion of the fluid equations made this kind of comparison possible.

Contents

Table of Contents	vi
List of Figures	viii
1 Introduction	1
2 Background	2
2.1 The Continuum Hypothesis	2
2.2 The Fluid Equations	3
2.3 Boundary Conditions	4
2.4 Poiseuille’s Law	5
2.5 Gas Dynamics	6
3 The Perturbative Expansion	8
3.1 The Poiseuille Limit	8
3.2 Results of the Expansion	10
3.2.1 0th Order	10
3.2.2 1st Order	10
3.2.3 2nd Order	11
4 Direct-Simulation-Monte-Carlo	12
4.1 Kinetic Theory	12
4.2 DSMC	13
4.2.1 Statistical Collisions	13
4.2.2 Particles in Cells	14
4.2.3 Boundary Conditions	14
4.3 FENIX	15
5 Results	17
5.1 Pressure	17
5.2 Temperature and Density	19
5.3 Flow Velocity	20
6 Conclusion	25

Bibliography 26

A The Poiseuille Expansion
– By Ross L. Spencer 27

List of Figures

5.1	Pressure Comparison	18
5.2	Radial Temperature Profile	19
5.3	Temperature Contour Plot	20
5.4	Density Contour Plot	22
5.5	Comparison of Velocity Profiles	23
5.6	Radial and Axial Velocity Profiles	24

Chapter 1

Introduction

The study of fluid behavior has been the source of many great advances in physics in the last centuries. Physicists of the early 1800's developed many of the techniques of vector calculus to model fluids. When James Clerk Maxwell formulated his combined theory of electricity and magnetism, he did so in the language of fluid mechanics. In our day and age of jet travel, nano-technology, and high-precision satellites, a proper understanding of the behavior of the fluids that surround and interact with these technologies is even more important.

To this end, several different methods have been developed to model fluid behavior. In the specific case of a gas, we will examine two of these methods: the Navier-Stokes fluid equations, and Direct-Simulation Monte Carlo. We will apply these both to the simple case of Poiseuille flow: steady flow of a gas through a cylindrical pipe. In the end, we will compare the results we obtain from these two highly distinct treatments of a fluid, and find that they are in excellent agreement. We will also develop formulas that yield results that are approximately correct.

Chapter 2

Background

The purpose of this work is to discuss the behavior of compressible fluid flow through a pipe, so it is important to have some understanding of the nature of a fluid. A fluid is defined as a material that will take the shape of its container, such as a liquid or a gas. At a microscopic level, fluids are simply conglomerates of molecules, interacting with each other through basic forces. Water is made up of H_2O molecules, argon is made of Ar atoms, and they interact through electrostatic forces generated by their nuclei and electron clouds. This description is conceptually very simple; all we need is classical electrodynamics and a simple molecular model. Unfortunately, once we extend our system to include more than a handful of molecules, it becomes very complex. To deal with this, we can make one of several approximations.

2.1 The Continuum Hypothesis

The most common approximation is to ignore the molecular nature of the fluid altogether, and instead treat it as a continuum. When we do this, we ignore the fluid's microscopic behavior, and only examine spatial and temporal averages of molecu-

Table 2.1 Variables Used and their Definitions

Variable	Quantity		
ρ	mass density	\vec{u}	vector flow velocity
n	number density	T	temperature
μ	coefficient of viscosity	k_B	Boltzmann's constant
P	thermodynamic pressure	ε	internal energy
λ	mean free path	m	molecular mass
κ	thermal conductivity	R	maximum value of r

lar quantities. For example, random particle motion is represented as temperature, trends in particle motion become flow velocities, and so on. This is acceptable, as long as the smallest volume scale we are interested in contains enough molecules for these averages to make sense. For gases, the Knudsen number is defined as the ratio of the mean free path of a molecule to the length scale of interest, and tracks the degree to which averaging is valid. In practice, a gas can be treated as a continuum if the Knudsen number is less than 0.1 [1].

2.2 The Fluid Equations

In fluid mechanics, there is no generally accepted notation for physical quantities. With that in mind, I will use variables as defined in table 2.1, to which I refer the reader. Unless otherwise noted, all quantities are assumed to be in SI units. The behavior of a continuous, electrically neutral fluid in the absence of external forces is described by a set of three coupled differential equations known as the fluid

equations. [2]

$$\frac{\partial \rho}{\partial t} + \nabla \cdot (\rho \vec{u}) = 0 \quad (2.1)$$

$$\rho \left(\frac{\partial u_i}{\partial t} + \vec{u} \cdot \nabla u_i \right) = -\frac{\partial P}{\partial r_i} + \frac{\partial}{\partial r_j} d_{ij} \quad (2.2)$$

$$\frac{\partial \varepsilon}{\partial t} + \vec{u} \cdot \nabla \varepsilon = \frac{1}{\rho} \left(-P \delta_{ij} + d_{ij} \frac{\partial u_i}{\partial r_j} \right) : \nabla \vec{u} + \frac{1}{\rho} \nabla \cdot (\kappa \nabla T) \quad (2.3)$$

where $d_{ij} = \mu \left(\frac{\partial u_i}{\partial r_j} + \frac{\partial u_j}{\partial r_i} - \frac{2}{3} \delta_{ij} \nabla \cdot \vec{u} \right)$ is the viscous stress tensor.

These equations, together with a thermodynamic equation of state and appropriate boundary conditions, completely describe the fluid.

2.3 Boundary Conditions

Boundary conditions for fluids are very important. Pressure, temperature and flow velocity must be defined at all boundaries, and this must be done in a self-consistent way, or no solution will exist for the system. In our case, we examine a long, cylindrical tube of radius $r = R$. We use cylindrical coordinates (r, ϕ, z) and assume the flow to be axisymmetric. The tube is open at both ends, where we specify a temperature and a pressure as well as flow velocities. Because of its length, u_ϕ and u_r must be zero far from the ends, and if we focus on that central region, we can assume $\vec{u} = u_z$ at all points in our problem.

We require that axial velocity at the solid wall (u_z) satisfy: [3]

$$u_z(R) = 1.11\lambda \left. \frac{\partial u_z}{\partial r} \right|_{r=R} \quad (2.4)$$

where λ is the mean free path of a molecule, or the average distance a molecule will travel between interactions with other molecules. For liquids and dense gases, we can effectively say $\lambda \approx 0$, so that $u_z(R) = 0$. We also require that the temperature of the gas be equal to the temperature of the tube at $r = R$.

Finally, we are interested in steady-state solutions, so all variables are considered to be independent of time (t).

2.4 Poiseuille's Law

In the case of a liquid, ρ is almost completely independent of both pressure and temperature. Under this simplification, the energy equation decouples, and (2.1) and (2.2) can be solved exactly for the case of steady flow in a long, cylindrical pipe. If we rewrite these equations in cylindrical coordinates under the assumptions given above, we have:

$$\begin{aligned} 0 &= u_\phi \\ 0 &= \frac{\partial u_z}{\partial z} + \frac{1}{r} \frac{\partial}{\partial r} (r u_r) \\ u_r \frac{\partial u_r}{\partial r} + u_z \frac{\partial u_r}{\partial z} &= -\frac{\partial P}{\partial r} + \mu \left(\nabla^2 u_r - \frac{u_r}{r^2} \right) \\ u_r \frac{\partial u_z}{\partial r} + u_z \frac{\partial u_z}{\partial z} &= -\frac{\partial P}{\partial z} + \mu \nabla^2 u_z \end{aligned}$$

In the simplest case where $u_r = 0$, these equations simplify dramatically:

$$\begin{aligned} 0 &= \frac{\partial u_z}{\partial z} \\ 0 &= -\frac{\partial P}{\partial r} \\ u_z \frac{\partial u_z}{\partial z} &= -\frac{\partial P}{\partial z} + \mu \nabla^2 u_z \end{aligned}$$

From this, we learn several important things about the flow of a liquid in a narrow pipe. First, u_z is a function of r only, and P is likewise a function of z only. Second, u_z and P must also satisfy the equation:

$$\frac{\partial P(z)}{\partial z} = \mu \frac{1}{r} \frac{\partial}{\partial r} \left(r \frac{\partial u_z(r)}{\partial r} \right) \quad (2.5)$$

Since the left-hand side depends only on z and the right-hand side depends only on r , it follows that each must independently be constant, and we have

$$P = P_0 + P'z \quad ,$$

where P_0 and P' are constants. P' can be easily found by comparing pressures for two values of z . From this, and applying the boundary condition $u_z(R) = 0$, we can see

$$u_z(r) = -P' \frac{1}{4\mu} (R^2 - r^2) \quad (2.6)$$

This is Poiseuille's law for flow of an incompressible fluid in a long, thin pipe.

2.5 Gas Dynamics

Poiseuille's Law was first obtained hundreds of years ago. However, when we tackle the same problem for the case of a gas, it becomes much more complicated, and an exact, analytical solution no longer exists. We examine the same situation as before, only this time we require that ρ be related to P and T by the ideal gas law:

$$mP = \rho k_B T \quad (2.7)$$

We can immediately see one consequence of this change. An examination of the continuity Eq. (2.1) reveals that \vec{u} is no longer guaranteed to be constant in z , but will instead satisfy

$$0 = \frac{\nabla \rho}{\rho} \cdot \vec{u} + \nabla \cdot \vec{u} \quad (2.8)$$

Therefore, any gradient in density will require a corresponding nonuniformity in the flow.

Eqs. (2.2) and (2.3) for momentum and energy can also be rewritten, such that

the fluid equations for steady flow of an ideal gas become: [2]

$$0 = \frac{\nabla \rho}{\rho} \cdot \vec{u} + \nabla \cdot \vec{u} \quad (2.9)$$

$$\rho (\vec{u} \cdot \nabla) \vec{u} = -\nabla P + \nabla \cdot \mu \nabla \vec{u} + \frac{1}{3} \nabla (\mu \nabla \cdot \vec{u}) \quad (2.10)$$

$$(\vec{u} \cdot \nabla) T = -(\gamma - 1) T \nabla \cdot \vec{u} + \frac{m(\gamma - 1)}{\rho k_B} \left[\nabla \cdot (\kappa \nabla T) + d_{ij} \frac{\partial u_i}{\partial r_j} \right] \quad (2.11)$$

From this point, we can go no further analytically. Zheng et al. solved a similar system using complicated numerical solvers specifically designed to treat the fluid equations, but they restricted themselves to a short flow region. [3]

If we restrict ourselves to the limit where deviations from Poiseuille's law are small, however, it is possible to use a perturbation analysis to obtain approximate analytic results. This approach will be discussed in Chapter 3.

Chapter 3

The Perturbative Expansion

Perturbation theory is a venerable method for solving complicated systems approximately. In essence, it works by adapting a known solution to a related system, rather than finding a new one from scratch. Here, we examine the application of perturbation theory to the fluid equations (2.9) under the boundary conditions appropriate to our cylindrical system.

3.1 The Poiseuille Limit

Before discussing the perturbative expansion itself, it is helpful to examine the Navier-Stokes equation for conservation of momentum more closely (2.10).

$$\rho (\vec{u} \cdot \nabla) \vec{u} = -\nabla P + \nabla \cdot \mu \nabla \vec{u} + \frac{1}{3} \nabla (\mu \nabla \cdot \vec{u})$$

This equation consists of four primary terms as shown here, each of which has a specific physical interpretation when applied to a microscopic element of fluid. From left to right, these are:

- **Inertial Momentum** This term represents the rate of change of fluid momentum that is present because the flow is nonuniform.

- Pressure Momentum This term represents the change in momentum that comes from a pressure imbalance across the fluid element.
- Viscous Momentum These two terms represent the change in momentum imparted to the fluid element as a result of viscous forces.

In the case of Poiseuille flow, viscous effects dominate the system and the gas does not compress much, so we can think of our problem as a perturbation on incompressible flow in the same system:

$$0 = -\nabla P + \nabla \cdot \mu \nabla \vec{u}$$

which is equivalent to the equations we solved in 2.4 to derive Poiseuille's law. Notice that we will be moving from using mass density (ρ) to number density (n). This is simple, as long as we are dealing with only one species of gas where $\rho = nm$.

This expansion is straightforward, but algebraically intensive; the details are given in Appendix A, work by R. L. Spencer. The solution takes the form:

$$\begin{aligned} u_r &= 0 \\ u_z &= u_0 + \epsilon u_1 + \epsilon^2 u_2 + \dots \\ n &= n_0 + \epsilon n_1 + \epsilon^2 n_2 + \dots \\ T &= T_0 + \epsilon T_1 + \epsilon^2 T_2 + \dots \end{aligned}$$

where u is assumed to point in the z -direction, and ϵ is a small expansion parameter which is discussed in detail at the end of the Appendix. There it is found that ϵ is of order

$$\frac{\Delta n}{n_0} \frac{R^4}{\Delta z^2 \lambda^2}$$

where λ is the mean-free-path assuming density n_0 . Other variables, such as viscosity (μ) and thermal conductivity (κ), are also typically functions of temperature, and

expand in a similar way. Note that $\bar{\mu}$ and $\bar{\kappa}$ are the viscosity and thermal conductivity, respectively, in the background state having density n_0 and temperature T_0 .

3.2 Results of the Expansion

When we substitute these expansions into the fluid equations (2.9), and collect powers of ϵ , we find several interesting results.

3.2.1 0th Order

To 0^{th} order, we recover a gas of constant density, pressure and temperature. Because viscous damping is present in the system, and we have no force to drive flow, we have:

$$u_0 = 0$$

$$P_0 = n_0 k_B T_0$$

3.2.2 1st Order

To first-order, we find several useful relations. From continuity, we find that u_1 is a function of r only, or that flow velocity does not change along the length of the pipe. The r -component of Eq. (2.10) tells us that P must be independent of r . We are free to choose ρ and T any way we like as long as they satisfy this, but the simplest choice is to have them both be independent of r as well. As in the case of a liquid, the z -component of (2.10) gives us

$$u_1 = -\frac{\Delta P}{\Delta z} \frac{1}{4\bar{\mu}} (R^2 - r^2 + 2.22\lambda R) \quad (3.1)$$

$$\Delta P = k_B (n_0 \Delta T + T_0 \Delta n) \quad (3.2)$$

where we have applied the boundary condition in Eq. (2.4). ΔP , Δn , and ΔT are the changes in quantities P , n , and T across the length of the pipe Δz .

Finally, Eq. (2.11) tells us that T_1 must be linear in z . Since P_1 is also linear in z , it follows that n_1 must be linear in z also. We may write this as

$$P_1 = n_0 k_B T_0 \left(\frac{\Delta n}{n_0} + \frac{\Delta T}{T_0} \right) \frac{z}{\Delta z}$$

So, we may drive this flow through a difference in density between the ends of the pipe, or a difference in temperature, or a combination of the two.

It is interesting to note that this exactly reproduces Poiseuille's law (2.6), except that we have applied a different boundary condition on u_z at $r = R$.

3.2.3 2nd Order

The second-order expansion of these equations poses much greater algebraic difficulties than the first two. This is because viscosity and thermal conduction become important at this order, which immensely complicates the business of finding the second-order corrections to ρ and T . Fortunately, part of the correction to flow velocity can be found directly from the continuity equation, without taking into account second-order effects of viscosity thermal conduction. It gives

$$u_2 = -\frac{\Delta P}{\Delta z} \frac{1}{4[\bar{\mu}]} (R^2 - r^2 + 2.2R\lambda) \left[-\frac{\Delta n}{\Delta z} \frac{z}{n_0} \right]. \quad (3.3)$$

Perturbation theory has then given us an approximate solution to the problem of flow in our geometry. This can be used in general application to gas flow in pipes, and it can also be specifically applied as a way to check the solution given to us by a completely different method.

Chapter 4

Direct-Simulation-Monte-Carlo

Although the fluid approximation is the most common way to deal with the complex behavior of a gas, it is by no means the only way. In this chapter, we will introduce the Direct-Simulation Monte Carlo (DSMC) algorithm as an alternative method for determining the behavior of a low-density gas.

4.1 Kinetic Theory

In Chapter 2 we talked briefly about the physical description of a gas as a collection of molecules, and the continuum approximation for simplifying the complex mathematics that result. Alternatively, we can leave the gas as a collection of molecules and instead simplify their interactions. We replace the complex electrostatic dipole interactions with some other form of “collision,” and apply basic scattering theory. One of the more basic collision models treats the gas molecules as perfectly elastic spheres. We can think of this as a collection of marbles (or billiard balls, to use the more traditional example) that bounce around in a box. Perhaps surprisingly, this rather naive model reproduces the behavior of a gas remarkably well. The introduc-

tion of more sophisticated collision models allows us to independently reproduce the physical properties of gases, such as viscosity. Perhaps the most important feature of this method is that it is not bound by the Knudsen number, as the fluid approximation is; it continues to work well, even at near-vacuum densities. In fact, it is in the realm of low-density gases where this method truly shines.

4.2 DSMC

The computational implementation of DSMC is remarkably straightforward. First, molecules move, and then they collide, changing their velocities. Repeat as needed. However, there are a few characteristics of this algorithm that bear mentioning.

4.2.1 Statistical Collisions

Unfortunately, the process of tracking the motion and collision details of a large number of molecules quickly becomes difficult. The best computers available can only handle a few thousand molecules this way. To remedy this, DSMC abandons an exact description of the system, and computes collisions statistically. Particles that are near one another are considered to have a certain probability of colliding, and a random number generator is used to determine if they in fact do. Particles that collide have their velocities changed as a result, in accordance with the proper statistical collision model. In this way, a computer can handle far larger numbers of molecules. We make a trade-off, however, in statistical noise, especially in regions with few collisions.

4.2.2 Particles in Cells

Our discussion in the previous section begs the question, “How does the computer determine which molecules are ‘near one another?’” Although there are many ways of answering this, one method that works well is to divide the simulation region into small collision cells. Any molecules that are found in the same cell are considered to be close enough to potentially collide. For this to make physical sense, the cells must be very small, on the order of the mean free path of the molecules. This is the reason that this method is best-suited to treating low-density gases; at high densities, the collision cells must be so small and so numerous that computers run out of memory.

In our cylindrical problem, the most natural way to divide the region is along uniformly-spaced lines of constant r and z , assuming cylindrical axisymmetry. This method has one major flaw: the volume of each cell is proportional to the radial position of the cell. This means that cells close to the axis will have a much smaller volume, and hence many fewer molecules than cells far from the axis. Because of this, we are forced to make another trade-off. We can either simulate many more particles than necessary at large radius, or we can allow the axial region to have fewer than necessary, and thus allow the gas to do unphysical things in that part of the simulation. Normally, we make some sort of compromise, getting many particles near the outer radius, and ignoring strange physical behavior near the axis. We also typically abandon a completely uniform grid, and define cells that are wider in r near the axis.

4.2.3 Boundary Conditions

As was the case with the fluid equations, we must also specify boundary conditions for DSMC. Pressures, temperatures and velocities must be provided at simulation

boundaries. We must also define some algorithm for dealing with interactions between the gas molecules and solid surfaces that accounts for thermal conduction and friction.

There is a key difference between the way DSMC handles boundary conditions and the way that the fluid equations do. Whereas using inconsistent boundary conditions to solve the fluid equations will result in no solution, DSMC manages to find one anyway. Essentially, the algorithm finds a physical solution for the central regions, and then patches that together with whatever boundary conditions it has been given. As a practical matter, this means that all we have to do is give the simulation a reasonable guess for boundary conditions, and it will give us a real, physical solution for regions that aren't too close to these boundaries. This robustness is one of the most valuable characteristics of the algorithm.

4.3 FENIX

As part of research in conjunction with the Department of Chemistry, Dr. Spencer *et al* have developed a DSMC algorithm called FENIX for use in cylindrical geometry. It is specifically tailored to simulate argon using the variable-soft-sphere collision model proposed by Koura [4], and we use a cell grid in which the region near the axis is divided into larger cells than regions at larger radius. We have used FENIX to simulate the same situation as we explored in Chapter 3.

Because DSMC is a numerical algorithm, we must now choose values for temperature, density, and so on. In order to keep the mean free path long enough to be convenient for DSMC to work with, we choose the following mean values:

$$T \approx 5400 \text{ K}$$

$$n \approx 3.77 \times 10^{22} \text{ m}^{-3}$$

$$P \approx 0.3 \text{ atm}$$

$$R = 0.5 \text{ mm}$$

We choose to drive flow through a density gradient, keeping T constant at all boundary points. We choose our density gradient to give us relatively high-speed flow, $u_z \approx 300 \text{ m/s}$. Under these conditions, the speed of sound is

$$v_s = \frac{5}{3} \sqrt{\frac{k_B T}{m}} \approx 1770 \text{ m/s}$$

This leads to a Mach number of 0.170, so $M^2 \ll 1$, as required by the perturbation expansion.

Chapter 5

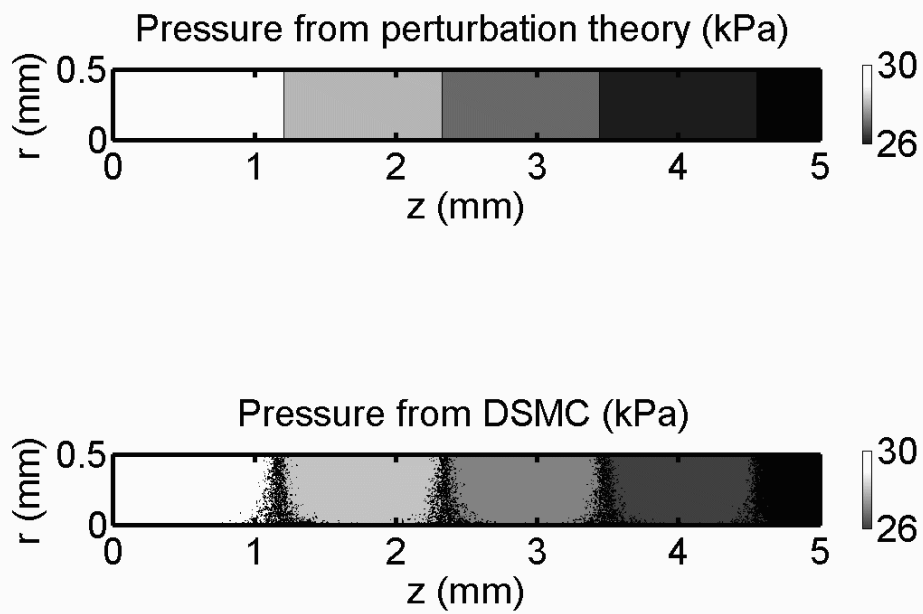
Results

Since we have now developed two completely separate methods of solving the problem of gas flow through a pipe, we now turn to a comparison of the results these two methods yield.

5.1 Pressure

Pressure is an important aspect of this problem, as it is the pressure gradient that actually drives the flow. one that keeps printing with a ridiculously tall colorbar. As we can see in Fig. 5.1, perturbation theory predicts a simple linear pressure gradient in z , and no r -dependence at all. DSMC reproduces this nearly exactly, aside from statistical noise, everywhere except near $r = 0$. This is a result of the small collision cells in that region, as discussed in section 4.2.2. This effect appears subtle here, but it becomes much more obvious when we examine temperature.

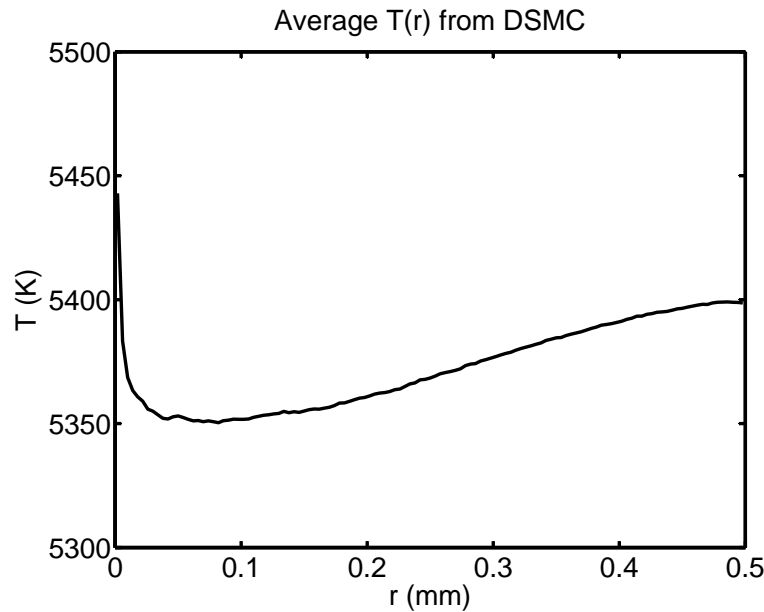
Figure 5.1 A comparison of pressure profiles from perturbation theory and from DSMC



5.2 Temperature and Density

The temperature of the gas is a measure of its kinetic energy, and is determined by the temperature at the boundaries, as well as viscous heating effects. According to first-order perturbation theory, under the boundary conditions we have provided, the gas should remain at a constant temperature of 5400 K. If we look at a plot of temperature as a function of radius, (Fig. 5.2) we see something very suspicious happening near the axis. At a radius of about 0.03 mm, the temperature suddenly

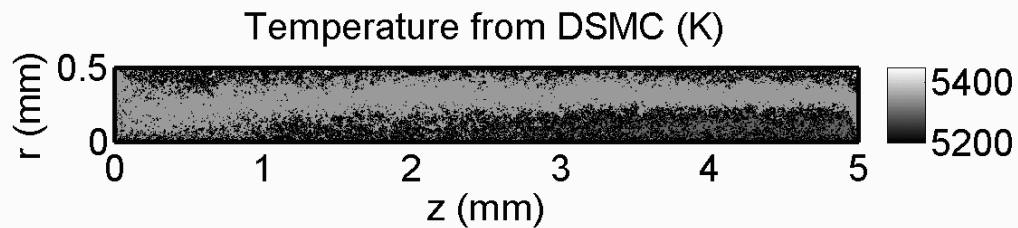
Figure 5.2 Average temperature as a function of radius as obtained from DSMC



spikes upward. This is the most obvious indicator that something is wrong with our results from DSMC near the axis. The trend toward higher temperatures near the wall of the tube, however, is real. Viscous heating, caused by frictional interactions between gas molecules, is less important near the axis. Because the wall is kept at a constant temperature of 5400 K, this forces the central region to be cooler, leading to a radial variation in temperature at second-order. The axial variation we see in Fig. 5.3 is an artifact of the naive boundary conditions we supplied at the ends.

We applied a constant radial profile in temperature, which then slowly dies out as we move downstream. If we instead load the ends with temperature profiles derived from second-order perturbation theory, this z -dependence of temperature should disappear. Regardless, the effect is small, and does not significantly affect the behavior of other variables. constant temperature gas we feed into the tube on the upstream end. This effect is small, and enters the perturbation expansion at second-order. This

Figure 5.3 Temperature profile from DSMC, showing radial variation and



same variation in temperature also affects the density of the gas, which adjusts to precisely cancel the radial variation introduced by temperature and maintain the pressure profile we have already seen. (Fig. 5.1)

5.3 Flow Velocity

The flow velocity provides the most detailed test we have. We know the corrections to u_z out to second order, and we can use these to compare profiles of velocity both in r and in z .

As we can see, the radial profile of velocity very closely follows the predicted value given by perturbation theory. We can see a clear deviation from parabolic behavior, however it is small. The predicted behavior when plotted along the z -axis also agrees remarkably well.

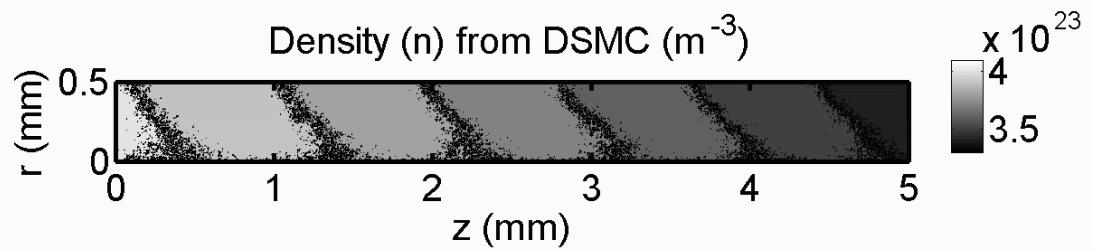
Figure 5.4 Density profile from DSMC

Figure 5.5 A comparison of velocity profiles from perturbation theory and DSMC

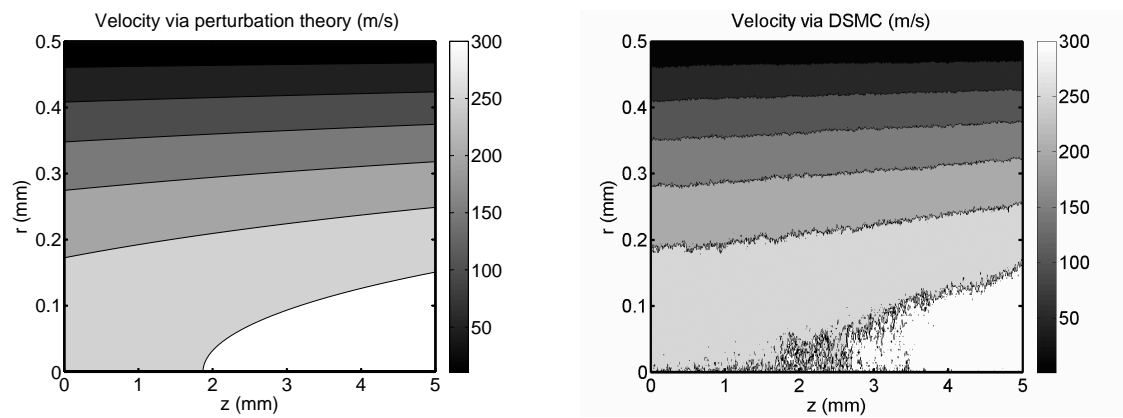
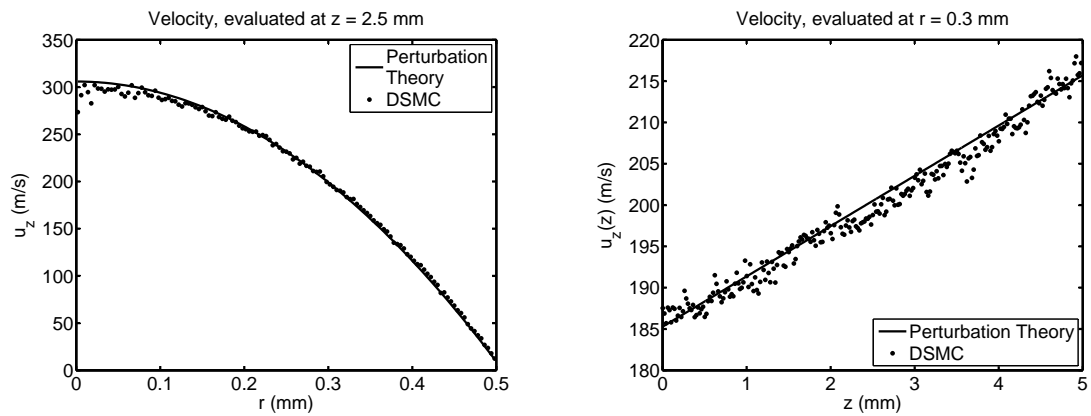


Figure 5.6 On the left we have a comparison of the radial variation of u_z between perturbation theory and the simulation; on the right a comparison of the axial variation.



Chapter 6

Conclusion

We have shown that, for the conditions we chose, the perturbative solution to the fluid equations and DSMC give very similar results. Even to first-order, we find only small differences in behavior. This leads us to believe that a perturbative solution that has been carried to second- or third-order will give excellent results for most Poiseuille-type flow, without the need for traditional computational fluid dynamics. These results also show that the FENIX implementation of DSMC correctly reproduces the physical behavior that we expect to find in a problem of this kind. Therefore, we can confidently apply FENIX to problems with much more complex geometries.

Bibliography

- [1] G. A. Bird, *Molecular Gas Dynamics and the Direct Simulation of Gas Flows*
- [2] T. Boyd and J. Sanderson, *The Physics of Plasmas*
- [3] Y. Zheng, A. L. Garcia, and B. J. Alder, “Comparison of Kinetic Theory and Hydrodynamics for Poiseuille Flow,” *Journal of Statistical Physics* **109**, 495–505 (2002).
- [4] K. Koura and H. Matsumoto, “Variable soft sphere molecular model for inverse-power-law or Lennard-Jones potential,” *Physics of Fluids A: Fluid Dynamics* **3**, 2459–2465 (1991).
- [5] M. N. Macrossan and C. R. Lilley, “Viscosity of argon at temperatures [greater-than] 2000 K from measured shock thickness,” *Physics of Fluids* **15**, 3452–3457 (2003).

Appendix A

The Poiseuille Expansion

– By Ross L. Spencer

As referenced in Sec. 3.1, we find in this appendix an approximate solution to the equations of gas dynamics for compressible gas flow in a pipe of length Δz and radius R driven by a pressure difference. Our coordinate system has $z = 0$ halfway between the two ends. There are, of course, many solutions to this problem corresponding to different boundary conditions at the inlet and the outlet of the pipe. What we seek is a solution that has vanishing radial velocity everywhere and that has “simple” dependence of u_z , n , and T on r and z , where by simple we mean that there is no rapid variation in z either at the inlet or at the outlet. We shall find a solution that depends only on relatively low powers of r and z , and which therefore, hopefully, represents the natural flow solution well away from both ends of the pipe.

We are interested in gas flow in which the viscous term in the Navier-Stokes equation is more important than the inertial term, i.e., gas flow in which the flow pattern is close to Poiseuille flow. (The precise meaning of this limit will be made clear at the end of the appendix.) In what follows we shall assume that the coefficients

of viscosity and thermal conduction are given by

$$\mu = \bar{\mu}(T/T_0)^\beta \quad , \quad \kappa = \bar{\kappa}(T/T_0)^\beta \quad , \quad (\text{A.1})$$

which is appropriate for monatomic gases such as argon, for which $\beta = 0.72$ to a good approximation. [5]

A suitable perturbation expansion that will be shown to produce such a solution is given by

$$n = n_0 + \epsilon n_1 + \epsilon^2 n_2 \quad (\text{A.2})$$

$$T = T_0 + \epsilon T_1 + \epsilon^2 T_2 \quad (\text{A.3})$$

$$u_z = \epsilon u_1 + \epsilon^2 u_2 \quad , \quad u_r = 0 \quad , \quad u_\theta = 0 \quad (\text{A.4})$$

where n_0 and T_0 are constants. This means that we are expanding about the very simple gas state in which density and temperature are constant and in which there is no flow. The pressure gradient applied along the length of the tube is treated as a first-order perturbation to which the gas responds.

Substituting this expansion into the gasdynamic equations shows that the uniform base state trivially satisfies the equations. The first-order equations are more interesting. They are as follows.

Continuity:

$$\frac{\partial}{\partial z}(n_0 u_1) = 0 \quad (\text{A.5})$$

Radial Navier-Stokes

$$0 = -k_B \left(T_0 \frac{\partial n_1}{\partial r} + n_0 \frac{\partial T_1}{\partial r} \right) + \frac{\bar{\mu}}{3} \frac{\partial^2 u_1}{\partial r \partial z} \quad (\text{A.6})$$

Axial Navier-Stokes

$$0 = -k_B \left(T_0 \frac{\partial n_1}{\partial z} + n_0 \frac{\partial T_1}{\partial z} \right) + \bar{\mu} \left[\frac{1}{r} \frac{\partial}{\partial r} \left(r \frac{\partial u_1}{\partial r} \right) + \frac{4}{3} \frac{\partial^2 u_1}{\partial z^2} \right] \quad (\text{A.7})$$

Energy:

$$0 = -\frac{2}{3} T_0 \frac{\partial u_1}{\partial z} + \frac{2\bar{\kappa}}{3n_0 k_B} \nabla^2 T_1 \quad (\text{A.8})$$

The boundary conditions are that n_1 and T_1 should produce a pressure difference Δp between the ends of the pipe and that $T_1(R, z)$, the temperature at the pipe, should either be zero (if the pressure difference is produced only by a density difference) or be a linear function of z if T_1 contributes to the pressure difference. The axial velocity at the wall must satisfy

$$u_1(R, z) = -\alpha \lambda \left. \frac{\partial u_1}{\partial r} \right|_{r=R} \quad (\text{A.9})$$

where $\alpha = 1.1$ and where λ is the mean-free-path of molecules in the zeroth-order state, $n = n_0$ and $T = T_0$. [3]

A solution to these first order equations can be found by considering them in order. First, the continuity equation requires that the first-order velocity only be a function of r : $u_1 = u_1(r)$. The radial component of the Navier-Stokes equation then requires that the first-order pressure,

$$P_1 = k_B(n_0 \Delta T + T_0 \Delta n) \quad , \quad (\text{A.10})$$

only depend on z . The simplest way to meet this requirement is to set $n_1 = n_1(z)$ and $T_1 = T_1(z)$. Other choices are possible but we are only trying to find one simple solution, so we make this choice.

The energy equation then requires that $T_1(z)$ be a linear function of z , and since the uniform state already has constant temperature we don't want to have an additive constant in T_1 . Hence

$$T_1 = \frac{\Delta T}{\Delta z} z \quad (\text{A.11})$$

where ΔT is the temperature change between the left and right ends of the pipe.

The axial component of the Navier-Stokes equation then consists of two terms, one of which is only a function of z and another which is only a function of r . In order for them to add to zero each must be a constant, which then requires that n_1 also be linear in z

$$n_1 = \frac{\Delta n}{\Delta z} z \quad (\text{A.12})$$

where Δn is the density change from the left end of the pipe to the right end.

The axial component of the Navier-Stokes equation can now be solved to obtain

$$u_1 = \frac{-k_B(n_0\Delta T + T_0\Delta n)}{4\Delta z\bar{\mu}}(R^2 + 2\alpha R\lambda - r^2) \quad (\text{A.13})$$

where we note that

$$-k_B(n_0\Delta T + T_0\Delta n) = \Delta P \quad , \quad (\text{A.14})$$

the pressure difference between the ends of the pipe. So we see that the first order flow is simply that predicted by Poiseuille's law, see Eq. (3.1)

We are now ready to proceed to second order. The second-order equations are

Continuity:

$$\frac{\partial}{\partial z}(n_0u_2 + n_1u_1) = 0 \quad (\text{A.15})$$

Radial Navier-Stokes

$$\begin{aligned} 0 = & -k_B \frac{\partial}{\partial r}(n_0T_2 + T_0n_2 + n_1T_1) + \frac{\bar{\mu}}{3} \frac{\partial^2 u_2}{\partial r \partial z} + \frac{\bar{\mu}\beta T_1}{3T_0} \frac{\partial^2 u_1}{\partial r \partial z} \\ & + \frac{\bar{\mu}\beta}{T_0} \left(-\frac{2}{3} \frac{\partial T_1}{\partial r} \frac{\partial u_1}{\partial z} + \frac{\partial T_1}{\partial z} \frac{\partial u_1}{\partial r} \right) \end{aligned} \quad (\text{A.16})$$

Axial Navier-Stokes

$$\begin{aligned} 0 = & -k_B \frac{\partial}{\partial z}(n_0T_2 + T_0n_2 + n_1T_1) + \bar{\mu} \left[\nabla^2 u_2 + \frac{1}{3} \frac{\partial^2 u_2}{\partial z^2} \right] + \frac{\bar{\mu}\beta T_1}{T_0} \left[\nabla^2 u_1 + \frac{1}{3} \frac{\partial^2 u_1}{\partial z^2} \right] \\ & - mn_0u_1 \frac{\partial u_1}{\partial z} + \frac{\bar{\mu}\beta}{T_0} \left[\frac{4}{3} \frac{\partial T_1}{\partial z} \frac{\partial u_1}{\partial z} + \frac{\partial T_1}{\partial r} \frac{\partial u_1}{\partial r} \right] \end{aligned} \quad (\text{A.17})$$

Energy:

$$\begin{aligned}
0 = & -u_1 \frac{\partial T_1}{\partial z} - \frac{2}{3} T_0 \frac{\partial u_2}{\partial z} - \frac{2}{3} T_1 \frac{\partial u_1}{\partial z} + \frac{2\bar{\kappa}}{3n_0 k_B} \nabla^2 T_2 + \frac{2\bar{\kappa}}{3n_0 k_B} \left(\frac{\beta T_1}{T_0} - \frac{n_1}{n_0} \right) \nabla^2 T_1 \\
& + \frac{2\bar{\kappa}\beta}{3n_0 k_B T_0} \left[\left(\frac{\partial T_1}{\partial r} \right)^2 + \left(\frac{\partial T_1}{\partial z} \right)^2 \right] + \frac{2\bar{\mu}}{3n_0 k_B} \left[\frac{4}{3} \left(\frac{\partial u_1}{\partial z} \right)^2 + \left(\frac{\partial u_1}{\partial r} \right)^2 \right] \quad (\text{A.18})
\end{aligned}$$

A relatively simple particular solution to these equations can be shown to be given by the following formulas:

$$u_2 = -\frac{n_1 u_1}{n_0} \quad (\text{A.19})$$

$$n_2 = \nu_{2r} r^2 + \nu_{4r} r^4 + \nu_{2z} z^2 \quad (\text{A.20})$$

with

$$\begin{aligned}
\nu_{2r} = & -\frac{\Delta n^2}{48\Delta z^2 n_0 \bar{\mu} \bar{\kappa}} (3n_0^2 T_0 k_B^2 (R^2 + 2\alpha\lambda R) + 4\bar{\mu} \bar{\kappa}) \\
& + \frac{\Delta n \Delta T}{96\Delta z^2 T_0 \bar{\mu} \bar{\kappa}} (3n_0^2 T_0 k_B^2 (R^2 + 2\alpha\lambda R) + 8\bar{\mu} \bar{\kappa} (3\beta - 1)) \\
& + \frac{-\Delta T^2 n_0}{32\Delta z^2 n_0 T_0^2 \bar{\mu} \bar{\kappa}} (3n_0^2 T_0 k_B^2 (R^2 + 2\alpha\lambda R) + 16\beta \bar{\mu} \bar{\kappa}) \quad , \quad (\text{A.21})
\end{aligned}$$

$$\nu_{4r} = \frac{n_0 k_B^2}{128\Delta z^2 T_0 \bar{\mu} \bar{\kappa}} (4T_0^2 \Delta n^2 + 3n_0 T_0 \Delta n \Delta T - n_0^2 \Delta T^2) \quad , \quad (\text{A.22})$$

and

$$\nu_{2z} = \frac{-1}{2\Delta z^2 n_0 T_0^2} (\Delta n^2 T_0^2 + (3 - \beta) n_0 T_0 \Delta n \Delta T - \beta n_0^2 \Delta T^2) \quad . \quad (\text{A.23})$$

$$T_2 = \tau_0 + \tau_{2r} r^2 + \tau_{4r} r^4 \quad (\text{A.24})$$

with

$$\tau_{4r} = -\frac{k_B \Delta p}{128\Delta z^2 \bar{\mu} \bar{\kappa}} (4T_0 \Delta n - n_0 \Delta T) \quad , \quad (\text{A.25})$$

$$\tau_{2r} = \frac{k_B^2(R^2 + 2\alpha R\lambda)}{32\Delta z^2 \bar{\mu} \bar{\kappa}} (2T_0^2 \Delta n^2 - n_0 T_0 \Delta n \Delta T - 3n_0^2 \Delta T^2) \quad , \quad (\text{A.26})$$

and

$$\tau_0 = -\tau_{2r} R^2 - \tau_{4r} R^4 \quad . \quad (\text{A.27})$$

Note that τ_0 is determined by the requirement that the second-order temperature vanish at the pipe since we have already satisfied the boundary conditions there in lowest and first order.

With these solutions in hand we may now find the meaning of our expansion parameter ϵ . Its simplest meaning can be found by requiring that n_1/n_0 and T_1/T_0 both be small. This simply requires

$$\frac{\Delta n}{n_0} \ll 1 \quad \frac{\Delta T}{T_0} \ll 1 \quad (\text{A.28})$$

We also note that the second-order comparison u_2/u_1 is also simple since $u_2/u_1 \simeq \Delta n/n_0$.

More interesting requirements are found, however, by looking at the ratios n_2/n_1 , and T_2/T_1 . We find

$$\frac{n_2}{n_1} \simeq \frac{1}{50} \frac{\Delta n}{n_0} \frac{R^4}{\Delta z^2 \lambda^2} \quad , \quad \frac{T_2}{T_1} \simeq \frac{1}{100} \frac{\Delta T}{T_0} \frac{R^4}{\Delta z^2 \lambda^2} \quad (\text{A.29})$$

That the ratios $\Delta n/n_0$ and $\Delta T/T_0$ appear is not surprising, but it is somewhat disconcerting to have the inverse of the Knudsen number, which is usually small, appear (λ^2 is in the denominator). The reason for this is that the coefficient of viscosity is proportional to λ , and if the viscosity becomes too small then the gas flow velocity will become too large for the flow to be Poiseuille-like.

For the numerical experiment reported in Sec. 5 these ratios are (over an axial subregion where end effects are negligible):

$$\frac{\Delta n}{n_0} = -0.05, \quad \frac{\Delta T}{T_0} = 0 \quad , \text{ and } \quad \frac{1}{50} \frac{\Delta n}{n_0} \frac{R^4}{\Delta z^2 \lambda^2} = -0.5 \quad . \quad (\text{A.30})$$

This error estimate is rather large, but for some reason the perturbation expansion fits the simulation data much better than expected.